

Electronic supplementary information for

**Graphene oxide interactions with co-existing heavy metal cations:
Adsorption, colloidal properties and joint toxicity**

Yang Gao^{a,b}, Xuemei Ren^{a,b,*}, Jianchun Wu^c, Tasawar Hayat^d, Ahmed Alsaedi^d, Cheng
Cheng^a, and Changlun Chen^{a,b,d,*}

^a*CAS Key Laboratory of Photovoltaic and Energy Conservation Materials, Institute of
Plasma Physics, Chinese Academy of Sciences, P.O. Box 1126, Hefei 230031, PR
China*

^b*Collaborative Innovation Center of Radiation Medicine of Jiangsu Higher Education
Institutions, Soochow University, Suzhou, 215123, PR China*

^c*Institute of Nuclear Science and Technology, Sichuan University, Chengdu 610064,
PR China*

^d*NAAM Research Group, King Abdulaziz University, Jeddah 21589, Saudi Arabia*

*Corresponding author. Tel: +86-0551-65592788, Fax: +86-0551-65591310

E-mail address: renxm1985@163.com (X.M. Ren); clchen@ipp.ac.cn (C.L. Chen)

The ESI contains 12 pages with 9 Figures and 3 Tables.

1 **Fig. S1** XPS characterization of GO. High resolution spectra of GO for C 1s peak (A)
2 and O 1s peak (B).

3 **Fig. S2** (A) AFM image of the GO sheets with (B) a corresponding AFM height
4 image.

5 **Fig. S3** Full FT-IR spectra of the GO, *E. coli* and *S. aureus*.

6 **Fig. S4** (A) Zeta potential and average size of GO as a function of pH; Relative
7 proportion of Cd(II) (B), Co(II) (C) and Zn(II) (D) species in solution as a function of
8 pH.

9 **Fig. S5** Intensity weighted size distribution of GO at pH = 6.0.

10 **Fig. S6** SEM images of *E. coli* (A, B), *E. coli* with 10 mg/L GO (C) and *E. coli* with
11 20 mg/L GO (D).

12 **Fig. S7** UV-Vis absorption spectroscopy of GO as a function of GO concentrations.
13 (A) Wavelength scan, and (B) Absorbance at 227 nm wavelength.

14 **Fig. S8** Exposures of *E. coli* and *S. aureus* to sterile Milli-Q water with increasing
15 time.

16 **Fig. S9** Exposures of *E. coli* (A) and *S. aureus* (B) to different concentrations of GO
17 with increasing time.

18

19 **Table S1** Curve fitting results of XPS C 1s spectrum

20 **Table S2** Curve fitting results of XPS O 1s spectrum

21 **Table S3** Physicochemical properties of the tested Me(II)

22

23

Bacterial cell membrane integrity assessment

In detail, bacterial cell suspension with 0.05 mmol/L Cd(II), 20 mg/L GO or 0.05 mmol/L Cd(II)+20 mg/L GO were added into individual well of a 24-well microplate (Greiner) and placed on a shaking incubator at 150 rpm for 2 h. Then, 10 μ L of mixture DNA dyes (SYTO9 : PI = 1 : 1) was added into the each well. The mixed solution was then dyed in the dark at room temperature for 30 min. The cell membrane integrity of bacterial was visualized by a laser scanning confocal microscope (Auriga, Zeiss, Germany) qualitatively. With the excitation wavelength centered at about 485 nm for both SYTO9 and PI, the fluorescence intensities at wavelengths centered at about 530 nm (green) and 630 nm (red) were measured, respectively. Different green-to-red fluorescence intensity ratios were proportional to different percentages of bacteria with intact cell membranes to those with damaged cell membranes.

Characterization methods and results

The sample for the FT-IR measurement was mounted on a BrukerEQinox55 spectrometer (Nexus) in a KBr pellet at room temperature. The average size of GO aggregates was measured by a Nanosizer ZS instrument (Malvern Instrument Co. Worcestershire, UK) operating with a He–Ne laser at a wavelength of 633 nm at 90° scattering angle. In these experiments, 1.25 mL achieved solution was added into the DLS cuvette. The cuvette was then placed into the light scattering unit for measurement. X-ray photoelectron spectroscopy (XPS) measurements were taken

1 using a VG Scientific ESCALAB Mark II spectrometer equipped with two ultrahigh
2 vacuum chambers. The AFM images were obtained in air using a Digital Instrumental
3 Nanoscope III in tapping mode. The morphology of the coating of GO on bacteria was
4 obtained by SEM (JSM-6700F) following a traditional procedure. Firstly, the treated
5 and untreated *E. coli* cells were fixed using 2.5% glutaraldehyde. The samples were
6 placed in a refrigerator overnight, washed three times with 0.1 M potassium
7 phosphate buffer (pH = 7.0), dehydrated using a graded series of ethanol (50%, 70%,
8 80%, 90%, 95%, and 100%) and pure acetone for 20 min.

9 The chemical composition and the element characterization of GO were measured by
10 X-ray photoelectron spectroscopy (XPS). The high-resolution C 1s and O 1s spectra
11 of GO are presented in Fig. S1A and B, respectively. The C 1s peak can be
12 decomposed into four components (Fig. S1A and Table S1). The peak at 284.66 eV
13 corresponds to C–C bond and its content is 60.67 %. The peaks located approximately
14 at 286.08 (4.06 %), 287.23 (32.08 %) and 288.97 (3.19 %) eV are the C–OH, C=O
15 and O–C=O bonds, respectively. As shown in Fig. S1B and Table S2, the O 1s peak
16 can be decomposed into three components. The content of C=O bond (at 532.96 eV)
17 takes up 60.68%, which demonstrates that oxygen atoms of GO exist in the form of
18 C=O bond dominantly. The peaks at 531.78 (17.09 %) and 533.53 (22.22 %) eV are
19 assigned to the O–C=O band and the C–OH bond, respectively. Based on the
20 elemental composition of GO determined by XPS, the ratio of carbon to oxygen (C/O)
21 is about 2.88 in GO, which is consistent with the previous study reported that the C/O
22 ratio of GO prepared by Hummer’s method is in the range of 2 – 3. The content of O

1 is 25.79 %, suggesting the considerable oxidation degree of GO by the oxidant during
2 its synthesis process.

3 Atomic force microscopy (AFM) is used to measure the thickness of the synthesized
4 GO nanosheets. The results are presented in Fig. S2A. The height image shown in Fig.
5 S2B indicates that the thickness of the GO sheets varies between 1.5 and 3 nm,
6 corresponding to approximately 1–3 layers. Fig. S2B also shows the sizes of GO
7 nanosheets are distributed in the range from 50 to 380 nm. There is a good correlation
8 between the nanosheet length as measured by AFM and the peak of the nanosheet size
9 distribution as outputted by the DLS instrument (68 to 458 nm as shown in Fig. S5).

10 Fig. S3 shows the full FT-IR spectra of GO, *E. coli* and *S. aureus*.

11 The zeta potential values of GO in the pH range from 1.5 to 11.0 are shown in Fig.
12 S4A. Note that the zero point charge of GO lies outside the pH range covered by the
13 curve. The zeta potential values of GO decrease with increasing pH values. At pH >
14 3.0, the zeta potential values of GO are less than –30 mV, resulting in the
15 electrostatically stable GO colloids. According to the results of our XPS
16 measurements (Fig. S1A and B), abundant oxygen-containing functional groups exist
17 on the GO nanosheets. Thus it is believed that the ionization of these
18 oxygen-containing functional groups leads to the increase in the negative charge on
19 the GO nanosheets, thereby generating a stable aqueous suspension due to the strong
20 electrostatic repulsion. Fig. S4A shows the average size of GO as a function of pH
21 value. GO average sizes are quite constant (~200 nm) from pH 3.0 to 11.0 and then
22 increase sharply as pH decreases from 3.0 to 1.5. These increased average size values

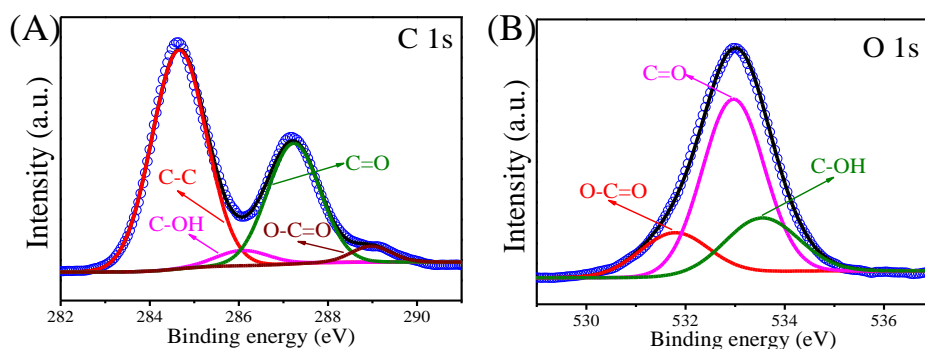
(>1000 nm) below pH 3.0 are due to a reduction in the hydrophilicity and negative charge of GO. The Cd(II), Co(II) and Zn(II) species are calculated by a chemical speciation model (Visual MINTEQ version 3.0) and the results demonstrate that Me(II) presents in the form of Me^{2+} , $\text{Me}(\text{OH})^+$, $\text{Me}(\text{OH})_2(\text{aq})$, and $\text{Me}(\text{OH})_3^-$ at various pH values (Fig. S4B–D). At pH < 8.0 , the predominant Me(II) species is Me^{2+} . Fig. S5 shows the intensity weighted size distribution of GO at pH = 6.0. The average size of GO is 210 nm and almost 90% of GO particles are distributed in the range from 105.7 to 295.3 nm.

SEM is employed to study the interactions between GO and bacteria. Fig. S6 shows the SEM images of *E. coli* cells before and after incubation with GO. As a control, Figs. S6A and B show the typical SEM images of native *E. coli* without GO, which exhibit the good preservation of the bacterial surfaces with obvious and coherent cytomembrane structures. A notable difference from the control group is that the surfaces of GO-treated bacterial cells become rough (Fig. S6C and D), suggesting the adhesion of many small GO fragments. This phenomenon suggests that a high concentration of GO can cover the external surface of cells, which might lead to indirect toxicity by biologically isolating them from the growth medium, and consequently the bacterial cells can neither proliferate nor consume nutrients or cation in the solution.

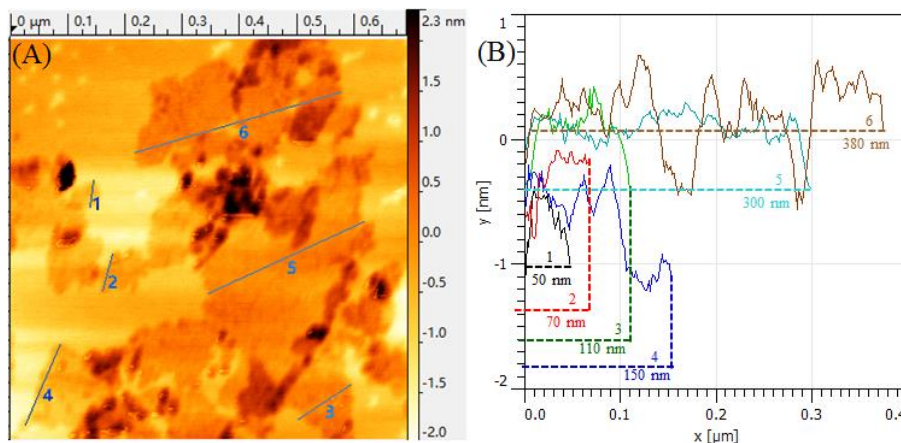
UV-Vis absorption spectroscopy of GO at different GO concentrations

The absorbance of GO is determined at different concentrations by UV-Vis

1 spectrophotometry (Shimadzu UV-2550). The corresponding results are presented in
 2 Fig. S7. The optimum wavelength of GO is determined to be 227 nm (Fig. S7A). An
 3 $R^2 > 0.99$ for the calibration curve of GO at 227 nm suggests that the GO absorbance
 4 are directly correlated to its concentrations (Fig. S7B).



7 **Fig. S1** XPS characterization of GO. High resolution spectra of GO for C 1s peak (A)
 8 and O 1s peak (B).



11 **Fig. S2** (A) AFM image of the GO sheets with (B) a corresponding AFM length and
 12 height image.

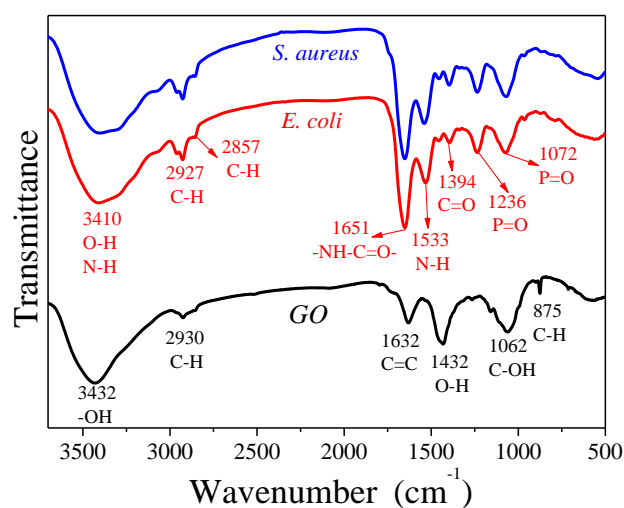


Fig. S3 Full FT-IR spectra of the GO, *E. coli* and *S. aureus*.

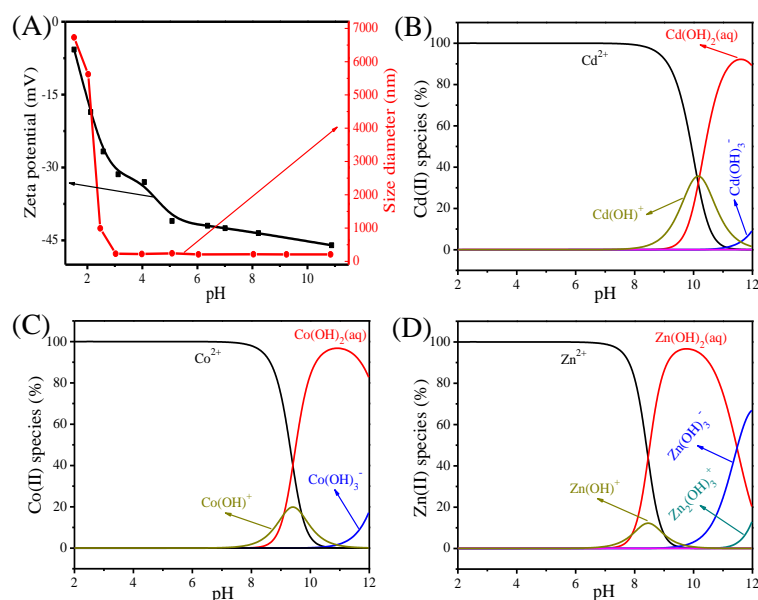


Fig. S4 (A) Zeta potential and average size of GO as a function of pH; Relative proportion of Cd(II)(B), Co(II)(C) and Zn(II)(D) species in solution as a function of pH.

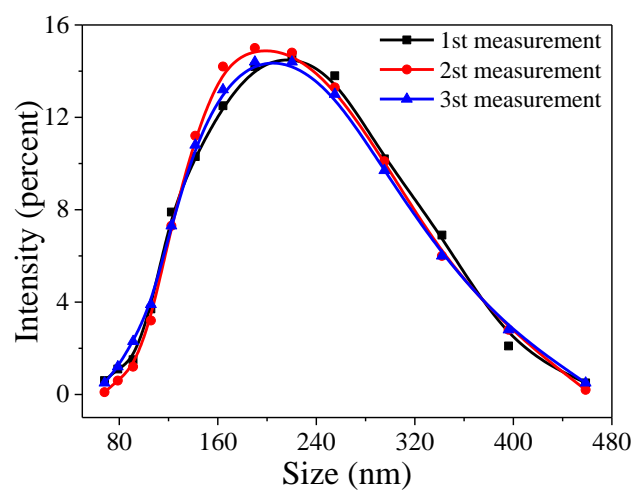


Fig. S5 Intensity weighted size distribution of GO at pH = 6.0.

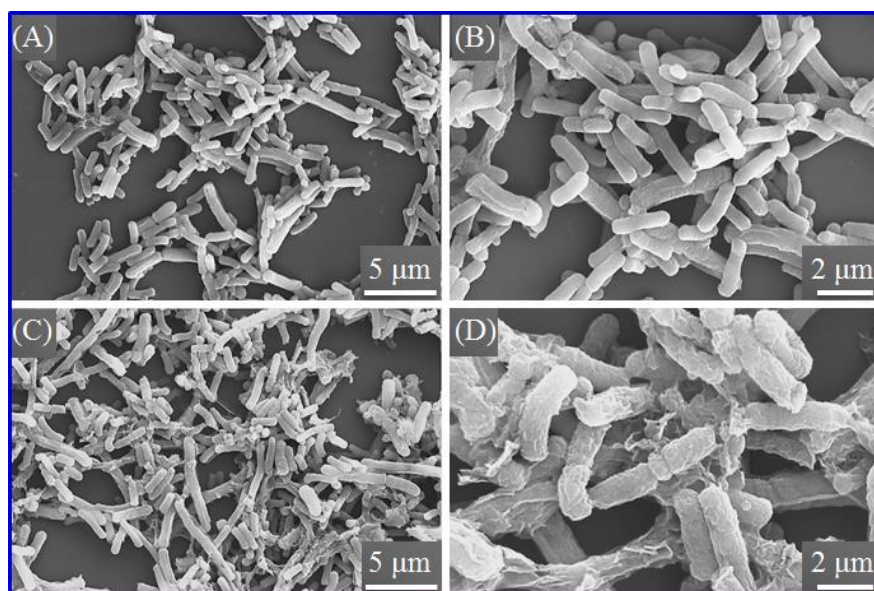


Fig. S6 SEM images of *E. coli* (A, B), *E. coli* with 10 mg/L GO (C) and *E. coli* with 20 mg/L GO (D).

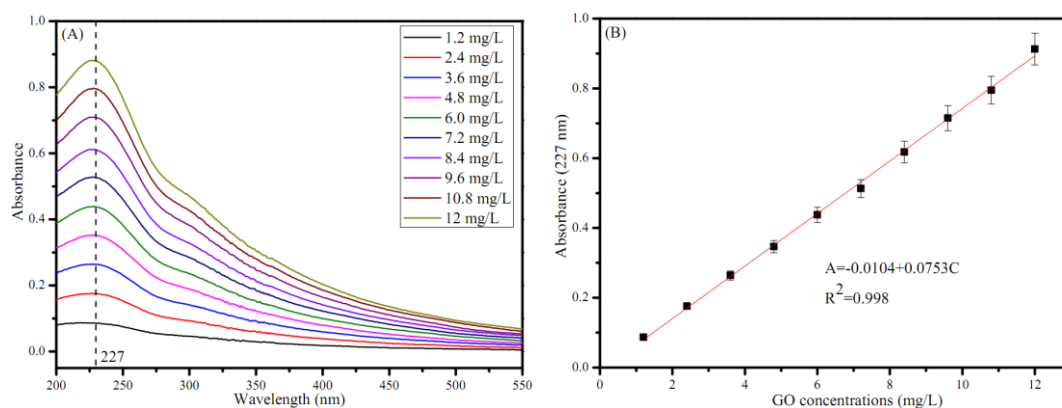


Fig. S7 UV-Vis absorption spectroscopy of GO as a function of GO concentrations.

(A) Wavelength scan, and (B) Absorbance at 227 nm wavelength.

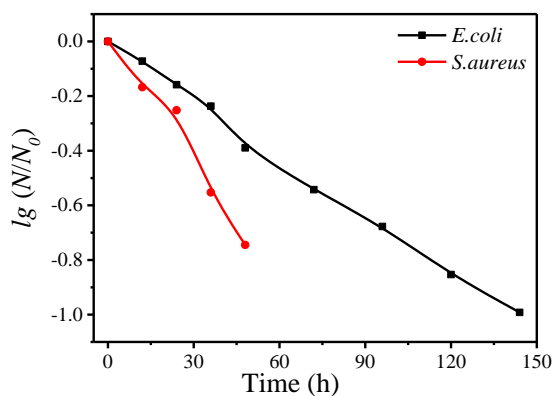


Fig. S8 Exposures of *E. coli* and *S. aureus* to sterile Milli-Q water with increasing time.

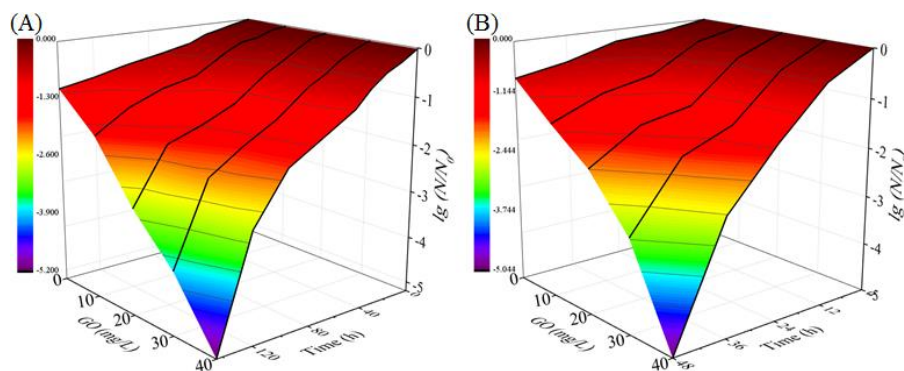


Fig. S9 Exposures of *E. coli* (A) and *S. aureus* (B) to different concentrations of GO with increasing time

1

Table S1 Curve fitting results of XPS C 1s spectrum

Peak	BE ^a (eV)	FWHM ^b (eV)	Area	%
C–C	284.66	1.52	41755.80	60.67
C–OH	286.08	1.20	2794.49	4.06
C=O	287.23	1.00	22077.28	32.08
O–C=O	288.97	0.50	2195.66	3.19

2

^a Binding energy; ^b Full width at half-maximum, C:O=2.543

3

4

5

Table S2 Curve fitting results of XPS O 1s spectrum

Peak	BE (eV)	FWHM (eV)	Area	%
O–C=O	531.78	1.64	9488.98	17.09
C=O	532.96	1.47	33683.07	60.68
C–OH	533.53	1.74	12335.67	22.22

6

7

Table S3 Physicochemical properties of the tested Me(II)^a

Metal	Mol. Wt.	Group	Electro-	R_{ionic}	R_{H}	HST	K_{sp}	pK_{h}
	(g/mol)		negativity	(Å)	(Å)	(Å)	(Me(OH) ₂)	
Co	58.93	VIII	1.88	0.79	4.23	3.44	1.09×10^{-15}	9.3
Zn	65.38	IIB	1.65	0.74	4.30	3.56	6.86×10^{-17}	8.2
Cd	112.41	IIB	1.69	0.97	4.26	3.29	5.27×10^{-15}	9.1

8

^a All properties from Ref 1–3.

9

10

1 Reference

2 1 K. J. Yang, B. L. Chen, X. Y. Zhu and B. S. Xing, *Environ. Sci. Technol.*, 2016, **50**,
3 11066-11075.

4 2 D. R Lide and H. P. Frederikse, *CRC handbook of chemistry and physics—A ready*
5 *book of chemical and physical data (78th ed.)*, CRC Press, New York, NY, 1998.

6 3 P. Trivedi, L. Axe and J. Dyer, *Colloids Surf. A*, 2001, **191**, 107-121.

7